

Oxygen Sorption and Catalytic Properties of $\text{La}_{1-x}\text{Sr}_x\text{Co}_{1-y}\text{Fe}_y\text{O}_3$ Perovskite-Type Oxides

H. M. ZHANG,* Y. SHIMIZU,* Y. TERAOKA,† N. MIURA,* AND N. YAMAZOE*¹

*Department of Materials Science and Technology, Graduate School of Engineering Sciences, Kyushu University, Kasuga, Fukuoka 816, and †Department of Industrial Chemistry, Faculty of Engineering, Nagasaki University, Nagasaki 852, Japan

Received May 31, 1989; revised September 12, 1989

Oxygen desorption from $\text{La}_{1-x}\text{Sr}_x\text{Co}_{1-y}\text{Fe}_y\text{O}_3$ perovskite-type oxides below 850°C was examined by a temperature-programmed desorption (TPD) technique. The catalytic activities of the oxides for the combustion of *n*-butane and methane as well as H_2O_2 decomposition in an alkaline solution were also measured and were discussed in relation to oxygen sorption properties. The amount of oxygen desorbed increased with increasing Sr content at a fixed B-site composition, for which an increase in the number of oxide ion vacancies with *x* was responsible. On the other hand, the total amount of oxygen desorbed was hardly affected by B-site composition, but partial substitution of Fe for Co enhanced desorption and sorption of oxygen particularly in the low-temperature region. Substitution of Sr for La as well as of Fe for Co was found to promote catalytic activity, though the activity changed with oxide composition in a manner dependent on the kind of reactant. For *n*-butane combustion over $\text{La}_{1-x}\text{Sr}_x\text{Co}_{0.4}\text{Fe}_{0.6}\text{O}_3$, maximum activity was obtained at $x = 0.2$. $\text{La}_{0.2}\text{Sr}_{0.8}\text{Co}_{1-y}\text{Fe}_y\text{O}_3$ activity was highest at $y = 0.4$ for *n*-butane combustion, while it was independent of *y* for methane combustion. For H_2O_2 decomposition in an alkaline solution, on the other hand, $\text{La}_{1-x}\text{Sr}_x\text{Co}_{0.4}\text{Fe}_{0.6}\text{O}_3$ and $\text{La}_{1-x}\text{Sr}_x\text{CoO}_3$ activities increased monotonically with an increase in *x*, and the former oxides were more active than the latter. These variations in catalytic activities with oxide composition were well accounted for by the oxygen sorption properties revealed by TPD. © 1990 Academic Press, Inc.

INTRODUCTION

Perovskite-type oxides represented by ABO_3 are known to show various functional properties, among which catalysis is one of the most important application fields. In 1970, Meadowcroft (1) reported that $\text{La}_{0.8}\text{Sr}_{0.2}\text{CoO}_3$ showed high catalytic activity comparable to that of platinum catalyst for the electrochemical reduction of oxygen. This finding triggered many studies, and perovskite-type oxides containing transition metals at B sites have been proven to be effective catalysts not only for the electrode process (2) but also for the combustion of carbon monoxide and light hydrocarbons (3).

In perovskite-type oxides, the substitution of A- and/or B-site cations by foreign

metal cations brings about modification of catalytic properties. For instance, substitution of Sr for Nd in NdCoO_3 or for La in LaCoO_3 enhanced the catalytic activities for the electrochemical reduction of oxygen (4) or the combustion of propane, methane, and carbon monoxide (5), respectively. So far we have investigated the oxygen sorption properties and defect structure of perovskite-type oxides by using a temperature-programmed desorption (TPD) technique, and have reported that the catalytic properties of Co- and Mn-based perovskite-type oxides are well accounted for by the oxygen sorption properties (6, 7).

This paper reports the oxygen sorption properties of $\text{La}_{1-x}\text{Sr}_x\text{Co}_{1-y}\text{Fe}_y\text{O}_3$ perovskite-type oxides as examined by TPD, and their catalytic activities for the combustion of methane and *n*-butane as well as the decomposition of hydrogen per-

¹ To whom correspondence should be addressed.

oxide in an alkaline solution, which is a key reaction in the electrochemical reduction of oxygen.

EXPERIMENTAL

Preparation of Catalysts

Three series of La_{1-x}Sr_xCo_{1-y}Fe_yO₃ oxides—La_{1-x}Sr_xCoO₃ ($x = 0, 0.2, 0.4, 1.0$), La_{1-x}Sr_xCo_{0.4}Fe_{0.6}O₃ ($x = 0, 0.2, 0.4, 0.6, 0.8, 1.0$), and La_{0.2}Sr_{0.8}Co_{1-y}Fe_yO₃ ($y = 0.4, 0.6, 0.8, 1.0$)—were prepared from special-grade reagents of lanthanum, strontium, and cobalt acetates and iron nitrate. An aqueous solution dissolving starting materials in a proportion of desired perovskite-type oxides was evaporated to dryness and then calcined at 850°C in air for 5–10 h. X-Ray diffraction analyses showed that all oxides except SrCoO_{2.5} had perovskite-type structure. SrCoO_{2.5} thus prepared contained a considerable amount of oxide ion vacancies crystallizing in brownmillerite-like structure (ABO_{2.5}) as reported before (8). The specific surface area of oxides was measured by the BET method (N₂ adsorption).

Temperature-Programmed Desorption of Oxygen

Each sample (0.5–1.0 g), after being mounted in a silica-glass reactor, was evacuated at 800°C for 1 h and then exposed to 13 kPa of oxygen for 1 h at a prescribed temperature (T_1), followed by cooling to room temperature (RT) in the same atmosphere. This oxygen sorption treatment is indicated as $T_1 \rightarrow$ RT hereafter, and unless stated otherwise T_1 is 800°C. After substitution of the atmosphere with a helium stream (60 cm³ min⁻¹), the sample was heated at a constant rate of 10°C min⁻¹ and the oxygen desorbed was monitored with a thermal conductivity detector. The preliminary experiment on La_{0.8}Sr_{0.2}Co_{0.4}Fe_{0.6}O₃ using a quadrupole mass spectrometer (Nichiden Varian TE-600) confirmed that the desorbed gas was only oxygen.

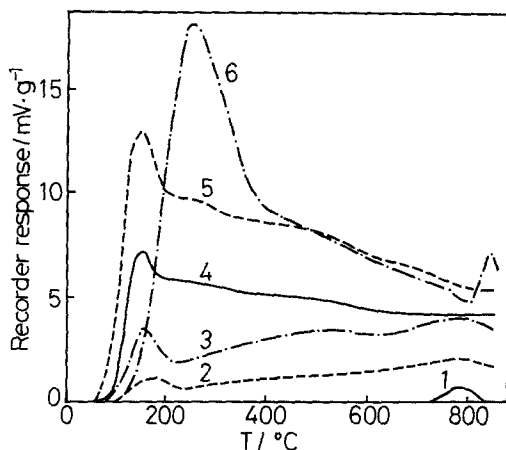


FIG. 1. TPD chromatograms of oxygen from La_{1-x}Sr_xCo_{0.4}Fe_{0.6}O₃ pretreated with oxygen at 800°C \rightarrow RT. (1) $x = 0$, (2) $x = 0.2$, (3) $x = 0.4$, (4) $x = 0.6$, (5) $x = 0.8$, (6) $x = 1.0$.

Combustion of *n*-Butane and Methane

The combustion reaction of *n*-butane and methane was carried out in a flow reactor. A gas mixture of *n*-butane (2.0 vol%) or methane (1.5 vol%), oxygen (20 vol%), and nitrogen (balance) was fed over the bed of 1 g catalyst. Carbon dioxide and water were the sole reaction products, and the carbon dioxide formed and the *n*-butane or methane reacted were analyzed by gas chromatography.

Decomposition of Hydrogen Peroxide

Catalysts (ca. 10 mg) were immersed in an aqueous solution of NaOH (9 M, 40 cm³) kept at 80°C, to which an aqueous solution of hydrogen peroxide (2 wt%, 5 cm³) was added under continuous stirring. The reaction rate was evaluated from the rate of oxygen evolution.

RESULTS

TPD of Oxygen

Figure 1 shows the TPD chromatograms of oxygen from La_{1-x}Sr_xCo_{0.4}Fe_{0.6}O₃, in which the ordinate (recorder response) corresponds to the rate of oxygen desorption.

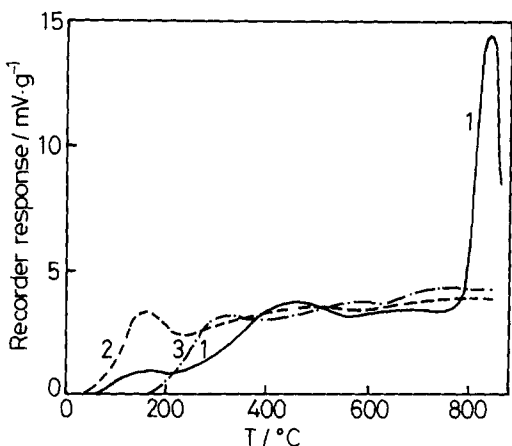


FIG. 2. TPD chromatograms of oxygen from $\text{La}_{0.6}\text{Sr}_{0.4}\text{Co}_{1-y}\text{Fe}_y\text{O}_3$ pretreated with oxygen at $800^\circ\text{C} \rightarrow \text{RT}$. (1) $y = 0$, (2) $y = 0.6$, (3) $y = 1.0$.

The oxygen desorption is seen to be a trace for $x = 0$ but increases sharply as x increases. It is noteworthy that the oxides with $x = 0.2$ – 0.8 or $x = 1.0$ show a desorption maximum at 150 or 250°C , respectively, and that Sr substitution for La enhances the oxygen desorption in such a low-temperature region. The amount of oxygen desorbed far exceeds a surface monolayer except at $x = 0$, indicating that the desorbed oxygen is liberated mostly from the oxide bulk. As stated later in detail, the desorbed oxygen is accommodated in the sites of oxide ion vacancies which are produced by the substitution of Sr for La. [In this sense, the oxides should be expressed by $\text{La}_{1-x}\text{Sr}_x\text{Co}_{1-y}\text{Fe}_y\text{O}_{3-\delta}$ (δ = oxygen deficiency). In this paper, however, a nominal formula $\text{La}_{1-x}\text{Sr}_x\text{Co}_{1-y}\text{Fe}_y\text{O}_3$ is used instead.]

Figure 2 shows how TPD chromatograms of oxygen vary with the composition of B-site cations (y) in $\text{La}_{0.6}\text{Sr}_{0.4}\text{Co}_{1-y}\text{Fe}_y\text{O}_3$ ($y = 0, 0.6, 1.0$). $\text{La}_{0.6}\text{Sr}_{0.4}\text{CoO}_3$ exhibited a sharp desorption peak centered around 820°C (β) in addition to a plateau-like peak appearing below 800°C (α), but Fe-containing oxides showed no sharp peaks corresponding to β desorption. It can be seen that the combination of Co and Fe at a B

site enhanced the oxygen desorption below ca. 300°C . This modification of the oxygen desorption behavior in the low-temperature region was more clearly observed on the oxides with higher Sr content, $\text{La}_{0.2}\text{Sr}_{0.8}\text{Co}_{1-y}\text{Fe}_y\text{O}_3$ (Fig. 3). In this oxide system, single-phase perovskite-type oxides were synthesized in the composition range $y \geq 0.4$. Although $\text{La}_{0.2}\text{Sr}_{0.8}\text{FeO}_3$ desorbed a large amount of oxygen, mixing of Fe with Co at the B site enhanced oxygen desorption in a low-temperature region and lowered the temperatures for the onset of oxygen desorption and for the desorption maximum; for $y = 0.6$ the lowest temperatures, 40°C (onset) and 150°C (peak maximum), were obtained, respectively. The amount of oxygen desorbed below 850°C was scarcely affected by the composition of Fe and Co (y).

Table 1 summarizes the amounts of desorbed oxygen determined by TPD after oxygen pretreatment ($T_1 \rightarrow \text{RT}$) where T_1 was set at 800°C , 300°C , or RT. Excepting $\text{LaCo}_{0.4}\text{Fe}_{0.6}\text{O}_3$ and $\text{La}_{0.6}\text{Sr}_{0.4}\text{CoO}_3$, desorption amounts as well as the profile of TPD chromatograms observed at $T_1 = 300^\circ\text{C}$ were essentially the same as those observed at $T_1 = 800^\circ\text{C}$. In addition, when pretreated with oxygen at RT, oxides having mixed B-site cations and a Sr content in the range $0.4 \leq x$

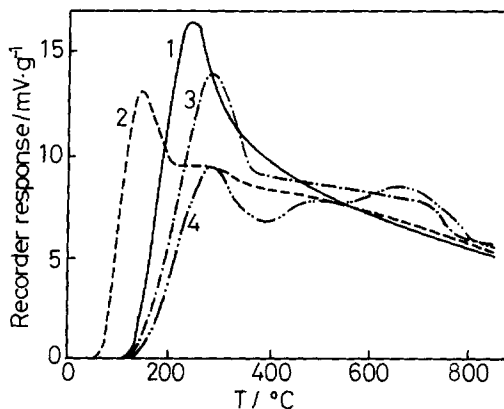


FIG. 3. TPD chromatograms of oxygen from $\text{La}_{0.2}\text{Sr}_{0.8}\text{Co}_{1-y}\text{Fe}_y\text{O}_3$ pretreated with oxygen at $800^\circ\text{C} \rightarrow \text{RT}$. (1) $y = 0.4$, (2) $y = 0.6$, (3) $y = 0.8$, (4) $y = 1.0$.

TABLE I

Effect of Oxygen Pretreatment Temperature on Amount of Oxygen Desorbed

Oxide	Amount desorbed ($\mu\text{mol g}^{-1}$) ^a		
	$T_1^b = 800^\circ\text{C}$	300°C	RT
LaCo _{0.4} Fe _{0.6} O ₃	12.1	5.3	1.3
La _{0.8} Sr _{0.2} Co _{0.4} Fe _{0.6} O ₃	116.5	106.4	78.5
La _{0.6} Sr _{0.4} Co _{0.4} Fe _{0.6} O ₃	282.9	278.9	275.6
La _{0.4} Sr _{0.6} Co _{0.4} Fe _{0.6} O ₃	444.7	456.4	448.3
La _{0.2} Sr _{0.8} Co _{0.4} Fe _{0.6} O ₃	756.3	761.0	757.8
SrCo _{0.4} Fe _{0.6} O ₃	759.0	763.2	491.8
La _{0.2} Sr _{0.8} Co _{0.6} Fe _{0.4} O ₃	785.0	792.7	744.8
La _{0.2} Sr _{0.8} Co _{0.2} Fe _{0.8} O ₃	755.9	763.6	745.9
La _{0.2} Sr _{0.8} FeO ₃	639.4	643.8	199.4
La _{0.6} Sr _{0.4} CoO ₃	207.3	151.6	78.5

^a Amount of oxygen desorbed below 800°C (α) for La_{0.6}Sr_{0.4}CoO₃ or below 850°C for other oxides.

^b Temperature at which oxygen pretreatment is started ($T_1 \rightarrow \text{RT}$).

≤ 0.8 desorbed a large amount of oxygen comparable to those observed at $T_1 = 800$ and 300°C . These results suggest that oxygen sorption proceeds easily and rapidly even at room temperature on the oxides with such mixed A- and B-site compositions.

Combustion of *n*-Butane and Methane

Figure 4 shows the temperature dependence of *n*-butane combustion on La_{1-x}Sr_x

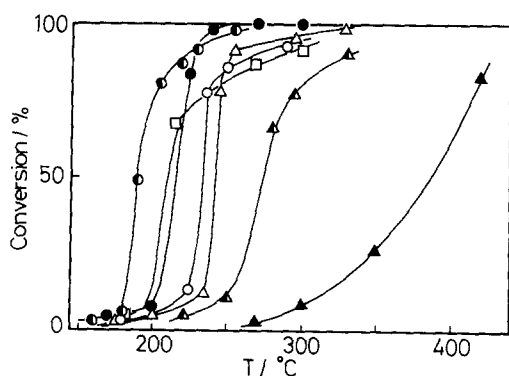


FIG. 4. *n*-Butane combustion over La_{1-x}Sr_xCo_{0.4}Fe_{0.6}O₃. ○, $x = 0$; ●, $x = 0.2$; ●, $x = 0.4$; △, $x = 0.6$; ▲, $x = 0.8$; ▲, $x = 1.0$; □, La_{0.6}Sr_{0.4}CoO₃.

Co_{0.4}Fe_{0.6}O₃. The activity depended largely upon Sr content, the order of which was $x = 0.2 > 0.4 > 0 > 0.6 > 0.8 > 1.0$. Note that La_{0.8}Sr_{0.2}Co_{0.4}Fe_{0.6}O₃ was even more active than La_{0.6}Sr_{0.4}CoO₃, which reportedly has the highest activity for *n*-butane oxidation in the La_{1-x}Sr_xCoO₃ system (6). The activity of La_{0.6}Sr_{0.4}CoO₃ was almost comparable to that of La_{0.6}Sr_{0.4}Co_{0.4}Fe_{0.6}O₃ in the present study. These results indicate that the partial substitution of Fe for Co is effective in increasing the catalytic activity.

Similar activity tests were carried out over La_{0.2}Sr_{0.8}Co_{1-y}Fe_yO₃ to see the effects of y . Arrhenius plots of the rates of *n*-butane and methane combustion are depicted in Fig. 5. The effects of B-site composition were different depending on the reactants. The *n*-butane combustion activity increased as $y = 1.0 < 0.6 < 0.8 < 0.4$, while methane combustion was hardly affected by the B-site composition.

Decomposition of Hydrogen Peroxide

In alkaline solutions, hydrogen peroxide (H₂O₂) exists as a form of hydrogen peroxide ion (HO₂⁻), and the decomposition reaction is written as

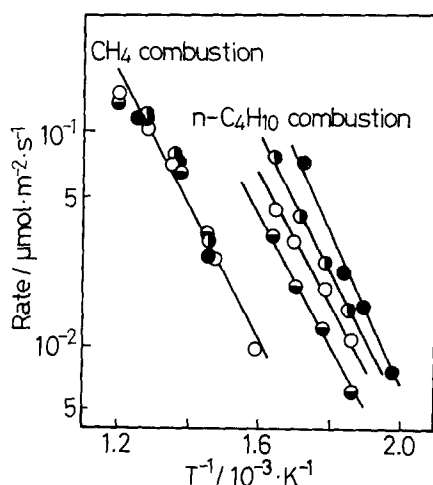
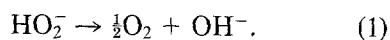


FIG. 5. Arrhenius plots of the rates of *n*-butane and methane combustion over La_{0.2}Sr_{0.8}Co_{1-y}Fe_yO₃. ●, $y = 0.4$; ○, $y = 0.6$; ●, $y = 0.8$; ○, $y = 1.0$.

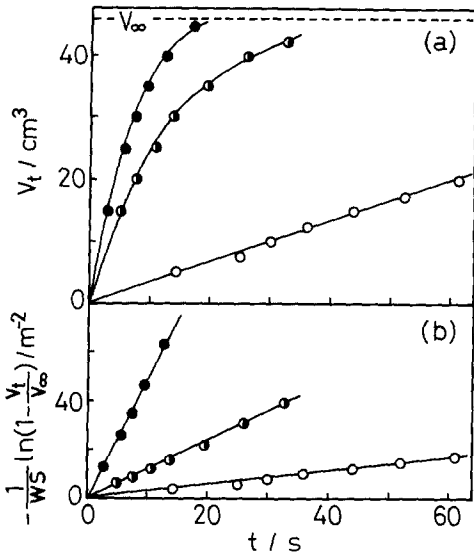


FIG. 6. H_2O_2 decomposition in an aqueous solution of 9 M NaOH at 80°C over $\text{La}_{1-x}\text{Sr}_x\text{Co}_{0.4}\text{Fe}_{0.6}\text{O}_3$. (a) Effect of time on the volume of evolved oxygen, V_t . (b) Verification of the first-order reaction. \circ , $x = 0$ (9.7 mg); \bullet , $x = 0.2$ (11.0 mg); \bullet , $x = 1.0$ (9.4 mg).

Catalytic decomposition of HO_2^- in an alkaline solution was carried out by suspending perovskite-type oxides in the solution. Figure 6a shows the effect of time on the volume of evolved oxygen (V_t). As we reported previously, the decomposition of HO_2^- on perovskite-type oxides is first-order with respect to HO_2^- concentration (10):

$$(1/WS)(dX/dt) = k_s(1 - X), \quad (2)$$

where X represents the conversion of HO_2^- , W the weight of the catalyst used (g), S the specific surface area of the catalyst [$\text{m}^2 \text{g}^{-1}$], and k_s the rate constant per unit surface area of the catalyst [$\text{s}^{-1} \text{m}^{-2}$], respectively. Integrating the equation and substituting (V_t/V_∞) for X gives

$$-(1/WS)\ln[1 - (V_t/V_\infty)] = k_s t \quad (3)$$

where V_t and V_∞ are the volumes (cm^3) of oxygen evolved to $t = t$ ($X = X$) and $t = \infty$ ($X = 1$), respectively. Therefore, a plot of $-(1/WS)\ln[1 - (V_t/V_\infty)]$ against t should be a straight line as shown in Fig. 6b and k_s is

determined as the slope of the plot. The catalytic activity of perovskite-type oxides for HO_2^- decomposition was evaluated by the k_s thus obtained. Figure 7 shows k_s values for two series of oxides, $\text{La}_{1-x}\text{Sr}_x\text{CoO}_3$ and $\text{La}_{1-x}\text{Sr}_x\text{Co}_{0.4}\text{Fe}_{0.6}\text{O}_3$, as a function of Sr content, x . In both series of oxides, the catalytic activity for HO_2^- decomposition increased with increasing x , though the activity of $\text{La}_{1-x}\text{Sr}_x\text{Co}_{0.4}\text{Fe}_{0.6}\text{O}_3$ was more dependent on x .

DISCUSSION

Oxygen Sorption Properties

Effects of A-site substitution. In a perovskite-type oxide LaMO_3 ($M =$ trivalent transition metal cation), the partial substitution of Sr^{2+} for La^{3+} requires charge compensation, which is achieved either by the formation of oxide ion vacancies, as shown by Eq. (4), or the formation of M^{4+} (or electron holes), as shown by Eq. (5). Equation (6) is the combination of (4) and (5):

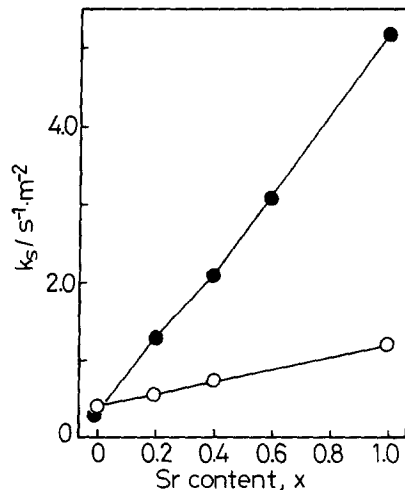
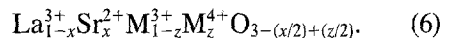
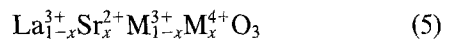
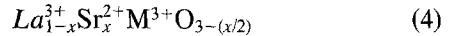


FIG. 7. Catalytic activity for H_2O_2 decomposition at 80°C of $\text{La}_{1-x}\text{Sr}_x\text{Co}_{0.4}\text{Fe}_{0.6}\text{O}_3$ (●) and $\text{La}_{1-x}\text{Sr}_x\text{CoO}_3$ (○).

TABLE 2
Amount of Oxygen Desorbed from
La_{1-x}Sr_xCo_{1-y}Fe_yO₃

Oxides	Surface area (m ² g ⁻¹)	Amount desorbed ^a		O/Sr ^c
		μmol g ⁻¹	θ ^b	
LaCo _{0.4} Fe _{0.6} O ₃	3.3	12.1	0.9	—
La _{0.8} Sr _{0.2} Co _{0.4} Fe _{0.6} O ₃	6.1	116.5	4.8	0.27
La _{0.6} Sr _{0.4} Co _{0.4} Fe _{0.6} O ₃	7.5	282.9	9.4	0.32
La _{0.4} Sr _{0.6} Co _{0.4} Fe _{0.6} O ₃	4.7	444.7	23.7	0.32
La _{0.2} Sr _{0.8} Co _{0.4} Fe _{0.6} O ₃	4.2	756.3	45.0	0.38
SrCo _{0.4} Fe _{0.6} O ₃	3.3	759.0	57.5	0.29
La _{0.2} Sr _{0.8} Co _{0.6} Fe _{0.4} O ₃	3.8	785.0	51.6	0.40
La _{0.2} Sr _{0.8} Co _{0.2} Fe _{0.8} O ₃	3.2	755.9	59.1	0.38
La _{0.2} Sr _{0.8} FeO ₃	3.2	639.4	50.0	0.32

^a Amount of oxygen desorbed below 850°C.

^b Surface coverage in unit of surface monolayer.

^c Amount of oxygen atoms desorbed per Sr atom.

We have reported (8) that when La_{1-x}Sr_xCoO₃ oxides are heated *in vacuo* or in a He stream up to ca. 800°C the charge compensation is achieved solely by the formation of oxide ion vacancies, Eq. (4). On cooling in an oxygen-containing atmosphere, the vacancies become occupied by absorbed oxygen to form tetravalent Co ions, Eq. (6). The oxide ions absorbed in this way can be discerned from the TPD chromatograms of oxygen as α desorption. These results allow us to mention that the sorption properties of α oxygen of perovskite-type oxides measured by a TPD technique reflect the nature of defect structure generated by the partial substitution.

On the other hand, β desorption from La_{1-x}Sr_xCoO₃ occurring as a sharp peak around 820°C corresponds to the reduction of some of the Co³⁺ to Co²⁺ (8). Such a β desorption peak was observed for La_{0.6}Sr_{0.4}CoO₃ (curve 1 in Fig. 2), but not for oxides with mixed B-site cations except for SrCo_{0.4}Fe_{0.6}O₃ (Figs. 1–3). This indicates that trivalent Co ions are stabilized by being mixed with Fe ions which are more resistant to reduction; LaFeO₃ is reportedly more stable than LaCoO₃ against decomposition in a reducing atmosphere (11).

The amounts of oxygen desorbed below 850°C from La_{1-x}Sr_xCo_{0.4}Fe_{0.6}O₃ and La_{0.2}Sr_{0.8}Co_{1-y}Fe_yO₃ are listed in Table 2. The amounts of oxygen desorbed far exceeded a surface monolayer except for the case of LaCo_{0.4}Fe_{0.6}O₃ (assuming 4.0 μmol O₂ m⁻² for one surface layer), indicating that the desorbed oxygen is liberated mostly from the bulk. Obviously, the amount of desorbed oxygen increased sharply with increasing *x*, while it remained almost unchanged with changing *y*. This dependence on the oxide composition agrees well with the nature of α oxygen mentioned above. That is, the amount of oxide ion vacancies is formally null for *x* = 0 and increases with the substitution of Sr²⁺ for La³⁺, but it is unaffected by the substitution of Fe³⁺ for Co³⁺. Thus the amount of α oxygen embedded at the sites of oxide ion vacancies is determined mostly by the A-site composition. The amount of desorbed oxygen atoms per Sr atom (O/Sr) is shown in the last column of Table 2. If α oxygen is associated with the oxide ion vacancies formed by the partial substitution of Sr²⁺ for La³⁺, O/Sr can take values between 0 and 0.5. In practice, O/Sr is seen to take ca. 0.4 for La_{0.2}Sr_{0.8}Co_{1-y}Fe_yO₃ (*y* = 0.4, 0.6, 0.8) and ca. 0.3 for others over a wide range of *x*. This allows us again to confirm the association of α oxygen with the oxide ion vacancies.

Effects of B-site substitution. As mentioned above, A-site composition affects mainly the amount of sorbed oxygen. On the other hand, B-site composition influences the properties of sorbed oxygen. As shown in Figs. 2 and 3, the partial substitution of Fe for Co clearly enhanced the oxygen desorption in the lower temperature region below ca. 300°C. It appears that the bonding strength of the sorbed oxygen is influenced by the composition of Co and Fe and becomes the weakest at *y* = 0.6 for La_{0.2}Sr_{0.8}Co_{1-y}Fe_yO₃.

The rapid and facile absorption of oxygen at lower temperature shown by Table 1 is also a marked promotion effect brought

about by the coexistence of Co and Fe at B sites. Oxides having mixed B-site cations and x in the range $0.4 \leq x \leq 0.8$ could absorb almost the same amounts of oxygen, even at room temperature, as those observed after $800^\circ\text{C} \rightarrow \text{RT}$ (Table 1). The absorption and desorption of oxygen accompany the redox changes of B-site cations between tetravalent and trivalent, as mentioned above. Accordingly, it is conceivable that the phenomena are somehow related to the relative ease of redox processes between $\text{Fe}^{4+} \rightleftharpoons \text{Fe}^{3+}$ and $\text{Co}^{4+} \rightleftharpoons \text{Co}^{3+}$. However, the effects of B-site mixing never seem to be so simple. The lowering of oxygen absorption temperature indicates that the rate process is largely promoted with mixed B-site cations of Co and Fe. The lowering of desorption temperature, on the other hand, suggests that part of the absorbed oxygen becomes less stable with the mixing of B-site cations. These effects should be explained in a future study.

A comment is added on the role of Fe substitution for Co on the crystal structure. It was reported that the upper limit of Sr content (x) for single-phase perovskite formation in the $\text{La}_{1-x}\text{Sr}_x\text{CoO}_3$ system was about 0.6 (12). In our study on the same system, a single-phase perovskite-type oxide was prepared at $x \leq 0.4$; oxides with $x = 1.0$ had a brownmillerite-like structure and oxides with $0.4 < x < 1.0$ were a mixture of perovskite and brownmillerite-like structures. In the Fe-containing oxides, however, perovskite structure could be maintained up to $x = 1.0$, in accordance with the previous report (13). Thus Fe substitution makes it possible to preserve perovskite structure up to the highest Sr content. Brownmillerite-like structure can be derived from the cubic perovskite structure by removing oxide ions regularly and thus ordering of oxide ion vacancies (14). We reported previously (8) that $\text{SrCoO}_{2.5}$ evacuated at 800°C has nearly cubic perovskite structure in which oxide ion vacancies are randomly distributed and that the anisotropic ordering of oxide ion vacan-

cies takes place with the sorption of α oxygen to give a brownmillerite-like structure. Consequently the presence of Fe ions at some B sites appears to suppress the ordering of oxide ion vacancies and thus preserves perovskite structure up to the highest Sr content, $x = 1.0$.

Catalytic Activity for Combustion Reactions

Effects of A-site substitution. Catalytic oxidation of light hydrocarbons over Co-based perovskite-type oxides proceeds by the redox mechanism (7, 15) in which oxide ions in the crystal lattice take part in the catalysis. We reported previously (6) that α oxygen was responsible for the high combustion activity of $\text{La}_{1-x}\text{Sr}_x\text{CoO}_3$ under the redox mechanism and that catalytic activity was determined by the amount and the reactivity of α oxygen. Figure 8 shows the amount of desorbed oxygen and the catalytic activity for *n*-butane combustion as a function of x in $\text{La}_{1-x}\text{Sr}_x\text{Co}_{0.4}\text{Fe}_{0.6}\text{O}_3$. The catalytic activity is expressed in terms of temperature at which the conversion of *n*-

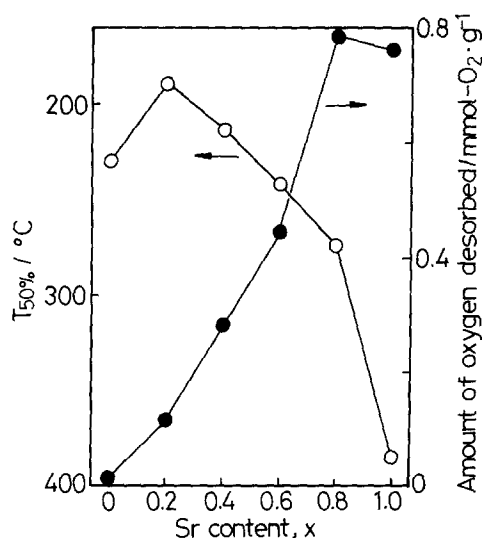


FIG. 8. Catalytic activity for *n*-butane oxidation (○) and amount of oxygen desorbed below 850°C (●) as a function of x in $\text{La}_{1-x}\text{Sr}_x\text{Co}_{0.4}\text{Fe}_{0.6}\text{O}_3$. $T_{50\%}$, temperature for 50% conversion of *n*-butane.

butane reaches 50% ($T_{50\%}$). It is seen that 20% substitution of Sr for La increases the activity while further substitution decreases the activity. On the other hand, the amount of desorbed oxygen monotonically increases with increasing x up to $x = 0.8$. These dependences found in La_{1-x}Sr_xCo_{0.4}Fe_{0.6}O₃ are essentially consistent with those found in La_{1-x}Sr_xCoO₃, though the highest activity of La_{1-x}Sr_xCoO₃ was obtained at $x = 0.4$ (6). Accordingly the change in catalytic activity with Sr substitution seems to be similarly accounted for by the dual effects of Sr substitution, i.e., an increase in the amount of active oxygen and a decrease in the reactivity of individual oxygen species. Because of these two opposing factors, catalytic activity seems to reach a maximum at a certain value of x (0.2 in the case of La_{1-x}Sr_xCo_{0.4}Fe_{0.6}O₃).

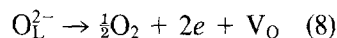
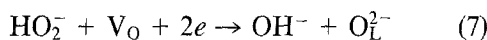
Effects of B-site substitution. As shown in Fig. 5, the effect of B-site composition, y , on the combustion activity of La_{0.2}Sr_{0.8}Co_{1-y}Fe_yO₃ differs with reactants; the activity was dependent on y in the n -butane combustion but not in the methane combustion. It has turned out that the changes in combustion activities with B-site composition are rather well related to the amount of α oxygen which remains in the oxides and is available to the reaction at the temperature of combustion reactions. The TPD chromatograms of oxygen from La_{0.2}Sr_{0.8}Co_{1-y}Fe_yO₃ (Fig. 3) are characterized by the appearance of a large desorption peak below 300°C. The temperatures of the n -butane combustion reaction, 200–300°C, are rather close to those of the large desorption peaks. The amounts of oxygen available at that temperature vary with y in the order $1.0 > 0.6 > 0.8 > 0.4$, which is in good accordance with the order of catalytic activity. In the temperature range of the methane combustion reaction, 350 to 500°C, on the other hand, the amount of α oxygen available to the reaction does not vary that much with y and this seems to explain the almost similar catalytic activities of the oxides. In contrast to the Sr sub-

stitution for La, the reactivity of individual oxygen species (α oxygen) seems to be affected little by the B-site substitution.

It is true that the partial substitution of Fe for Co clearly increases the catalytic activity for n -butane oxidation as typically illustrated by the superiority of La_{0.8}Sr_{0.2}Co_{0.4}Fe_{0.6}O₃ to La_{0.6}Sr_{0.4}CoO₃ (Fig. 4), but this promotion effect is likely due to mainly an increase in available oxygen.

Catalytic Activity for H₂O₂ Decomposition

The catalytic decomposition of H₂O₂ over an oxide catalyst in an alkaline solution is assumed to proceed by two steps



where V_O and O_L⁻ are oxide ion vacancy and lattice oxide ion, respectively. The electronic conductivity of La_{1-x}Sr_xCo_{1-y}Fe_yO₃ oxides is reported to be sufficiently high (16) that the charge transfer between the reactants and the catalyst may be too fast to control the total rate. Accordingly the decomposition rate should be determined by the amount of oxide ion vacancies (7) and/or the readiness of oxygen desorption (8). The activity for H₂O₂ decomposition at 80°C (Fig. 7) increased monotonically with increasing x in both oxide systems, La_{1-x}Sr_xCo_{0.4}Fe_{0.6}O₃ and La_{1-x}Sr_xCoO₃. Such monotonic increases are in good contrast to the cases of hydrocarbon oxidation activity in which Sr substitution has optimum values. Unlike hydrocarbon oxidation reactions, HO₂⁻ decomposition does not need association of reactive oxygen species, and this seems to result in the above monotonic increases. The promotion effects of Sr substitution can be explained in two ways. (1) The substitution increases the amount of oxide ion vacancies and thus increases the rate of (7). (2) The substitution increases the rate of oxygen desorption in the lower temperature region and thus increases the rate of (8). Of the two explanations, the latter appears to be more plau-

sible when the marked effects of the partial substitution of Fe for Co are considered.

The activity of $\text{La}_{1-x}\text{Sr}_x\text{Co}_{0.4}\text{Fe}_{0.6}\text{O}_3$ was always higher than that of $\text{La}_{1-x}\text{Sr}_x\text{CoO}_3$ when x was fixed. TPD results showed that Fe substitution enhanced oxygen desorption at temperatures below ca. 300°C (Fig. 2) and that an increase in oxygen desorption in this low-temperature region was more prominent in $\text{La}_{1-x}\text{Sr}_x\text{Co}_{0.4}\text{Fe}_{0.6}\text{O}_3$ (Fig. 1) as compared with the case of $\text{La}_{1-x}\text{Sr}_x\text{CoO}_3$ reported previously (6). Also revealed was that Fe-substituted oxides absorbed oxygen very easily, even at room temperature (Table I). Thus, enhancement of the rates of oxygen sorption-desorption in the low-temperature region seems to be most responsible for the promotion effect of Fe substitution in H_2O_2 decomposition.

Effects of Fe Substitution on Catalytic and Oxygen Sorption Properties

As stated above, substitution of Fe for Co was found to enhance oxygen sorption-desorption properties as well as catalytic activity for the combustion of hydrocarbons and H_2O_2 decomposition. The variation of catalytic activity with oxide composition was well accounted for by the oxygen sorption properties. Fe substitution enhanced oxygen desorption particularly at temperatures below ca. 300°C. In accordance, Fe substitution prominently promoted catalytic activity for H_2O_2 decomposition and n -butane combustion catalyzed at relatively low temperatures. In addition, Fe substitution was effective in preserving perovskite-type structure at higher Sr contents.

It has been reported that perovskite-type oxides with only Co at B sites are among the most active catalysts, while oxides with only Fe are less active for combustion reactions (5, 17, 18) or electrode processes (10, 19). The present study shows that oxides with mixed B-site cations can often be more active than oxides with unmixed B-

site cations. So far the catalytic activity of perovskite-type oxides has been studied mostly with regard to A-site substitution. However, the results obtained here suggest the possibility of finding more excellent catalysts by selecting the proper combination of not only A-site cations but also B-site cations.

REFERENCES

1. Meadowcroft, D. B., *Nature (London)* **226**, 847 (1970).
2. Tamura, H., Yoneyama, H., and Matsumoto, Y., in "Electrodes of Conductive Metallic Oxides, Part A" (S. Trasatti, Ed.), p. 261. Elsevier, Amsterdam, 1980.
3. Voorhoeve, R. J. H., in "Advance Materials in Catalysis" (J. J. Burton and R. L. Garten, Eds.), p. 129. Academic Press, New York, 1977.
4. Kudo, T., Obayashi, H., and Gejo, T., *J. Electrochem. Soc.* **122**, 159 (1975).
5. Nakamura, T., Misono, M., Uchijima, T., and Yoneda, Y., *Nippon Kagaku Kaishi*, 1679 (1980).
6. Teraoka, Y., Furukawa, S., Yamazoe, N., and Seiyama, T., *Nippon Kagaku Kaishi*, 1529 (1985).
7. Zhang, H. M., Teraoka, Y., and Yamazoe, N., *J. Surf. Sci. Soc. Japan* **8**, 23 (1987).
8. Yamazoe, N., Furukawa, S., Teraoka, Y., and Seiyama, T., *Chem. Lett.*, 2019 (1982).
9. Teraoka, Y., Yoshimatsu, M., Yamazoe, N., and Seiyama, T., *Chem. Lett.*, 893 (1984).
10. Miura, N., Shimizu, Y., Yamazoe, N., and Seiyama, T., *Nippon Kagaku Kaishi*, 644 (1985).
11. Nakamura, T., Petzow, G., and Gauckler, L. J., *Mater. Res. Bull.* **14**, 649 (1979).
12. Obayashi, H., Kudo, T., and Gejo, T., *Japan. J. Appl. Phys.* **13**, 1 (1974).
13. Matsumoto, Y., Yamada, S., Nishida, T., and Sato, E., *J. Electrochem. Soc.* **127**, 2360 (1980).
14. Wadsley, A. D., in "Non-stoichiometric Compounds" (L. Mandelcorn, Ed.), p. 134. Academic Press, New York/London, 1964.
15. Nakamura, T., Misono, M., and Yoneda, Y., *J. Catal.* **83**, 151 (1983).
16. Teraoka, Y., Okamoto, K., and Yamazoe, N., *Mater. Res. Bull.* **23**, 51 (1988).
17. Teraoka, Y., Tanoue, Y., Yamazoe, N., and Seiyama, T., *Eng. Sci. Rep. Kyushu Univ.* **6**, 9 (1984).
18. Arai, H., Yamada, T., Eguchi, K., and Seiyama, T., *Appl. Catal.* **26**, 265 (1986).
19. Miura, N., Shimizu, Y., and Yamazoe, N., *Nippon Kagaku Kaishi*, 751 (1986).